The Journal of Clinical Endocrinology & Metabolism, 2024, **109**, 858–867
https://doi.org/10.1210/clinem/dgad550
Advance access publication 15 September 2023
Clinical Research Article

Circulating miRNAs Detect High vs Low Visceral Adipose Tissue Inflammation in Patients Living With Obesity

Nataly Makarenkov,[1,2] Yulia Haim,[1] Uri Yoel,[1,3] Yair Pincu,[1] Tanya Tarnovscki,[1] Idit F. Liberty,[4] Ivan Kukeev,[5] Lior Baraf,[3] Oleg Dukhno,[5] Oleg Zilber,[6] Matthias Blüher,[7] Assaf Rudich,[1] and Isana Veksler-Lublinsky[2]

[1]Department of Clinical Biochemistry and Pharmacology, Faculty of Health Sciences, Ben-Gurion University of the Negev, Beer-Sheva 84103, Israel
[2]Department of Software & Information Systems Engineering, Faculty of Engineering, Ben-Gurion University of the Negev, Beer-Sheva 84103, Israel
[3]Endocrinology Unit, Soroka University Medical Center, Beer-Sheva 84101, Israel
[4]Diabetes Clinic, Soroka University Medical Center, Beer-Sheva 84101, Israel
[5]Department of General Surgery B, Soroka University Medical Center, Beer-Sheva 84101, Israel
[6]Goldman Faculty of Health Sciences, Ben-Gurion University of the Negev, Beer-Sheva 84103, Israel
[7]Helmholtz Institute for Metabolic, Obesity and Vascular Research (HI-MAG) of the Helmholtz Zentrum München at the University of Leipzig and University Hospital Leipzig, Leipzig 04103, Germany

Correspondence: Assaf Rudich, MD, PhD, Department of Clinical Biochemistry and Pharmacology, Faculty of Health Sciences, Ben-Gurion University of the Negev, Rager Blvd., Beer-Sheva 84103, Israel. Email: rudich@bgu.ac.il; or Isana Veksler-Lublinsky, PhD, Department of Software & Information Systems Engineering, Faculty of Engineering, Ben-Gurion University of the Negev, Rager Blvd., Beer-Sheva 84103, Israel. Email: vaksler@post.bgu.ac.il.

Abstract

Context: The severity of visceral adipose tissue (VAT) inflammation in individuals with obesity is thought to signify obesity subphenotype(s) associated with higher cardiometabolic risk. Yet, this tissue is not accessible for direct sampling in the nonsurgical patient.

Objective: We hypothesized that circulating miRNAs (circ-miRs) could serve as biomarkers to distinguish human obesity subgroups with high or low extent of VAT inflammation.

Methods: Discovery and validation cohorts of patients living with obesity undergoing bariatric surgery (n = 35 and 51, respectively) were included. VAT inflammation was classified into low/high based on an expression score derived from the messenger RNA levels of *TNFA*, *IL6*, and *CCL2* (determined by reverse transcription polymerase chain reaction). Differentially expressed circ-miRs were identified, and their discriminative power to detect low/high VAT inflammation was assessed by receiver operating characteristic–area under the curve (ROC-AUC) analysis.

Results: Fifty three out of 263 circ-miRs (20%) were associated with high-VAT inflammation according to Mann-Whitney analysis in the discovery cohort. Of those, 12 (12/53 = 23%) were differentially expressed according to Deseq2, and 6 significantly discriminated between high- and low-VAT inflammation with ROC-AUC greater than 0.8. Of the resulting 5 circ-miRs that were differentially abundant in all 3 statistical approaches, 3 were unaffected by hemolysis and validated in an independent cohort. Circ-miRs 181b-5p, 1306-3p, and 3138 combined with homeostatic model assessment of insulin resistance (HOMA-IR) exhibited ROC-AUC of 0.951 (95% CI, 0.865-1) and 0.808 (95% CI, 0.654-0.963) in the discovery and validation cohorts, respectively, providing strong discriminative power between participants with low- vs high-VAT inflammation. Predicted target genes of these miRNAs are enriched in pathways of insulin and inflammatory signaling, circadian entrainment, and cellular senescence.

Conclusion: Circ-miRs that identify patients with low- vs high-VAT inflammation constitute a putative tool to improve personalized care of patients with obesity.

Key Words: visceral adipose tissue inflammation, circulating miRNAs, biomarkers, next-generation sequencing, obesity subphenotyping

Abbreviations: AT, adipose tissue; AUC, area under the curve; BMI, body mass index; cDNA, complementary DNA; DEM, differentially expressed miRNA; HOMA-IR, homeostatic model assessment of insulin resistance; IL6, interleukin 6; miRNA, microRNA; mRNA, messenger RNA; NGS, next-generation sequencing; qPCR, quantitative polymerase chain reaction; RBC, red blood cell; ROC, receiver operating characteristic; RPM, reads per million; TNFα, tumor necrosis factor α; VAT, visceral adipose tissue; VIA-circ-miRs, VAT inflammation-associated circ-miRs.

Obesity is defined as adipose tissue (AT) accumulation to degrees that negatively affect health (1, 2). Yet, as currently defined anthropometrically using body mass index (BMI), obesity is still highly heterogeneous in its effect on health-related outcomes of affected patients (3). Cross-sectional studies repeatedly link visceral fat mass accumulation with worse cardiometabolic risk profile, and longitudinal studies suggest that surrogate parameters for preferential accumulation of visceral AT (VAT) (over subcutaneous fat) are associated with an increased risk of death (4). Yet, beyond fat mass per se, VAT inflammation is a major feature of "adiposopathy," or obesity-related AT disease (5), which is associated with dysfunctional AT and with a greater effect of obesity on health. Indeed, immune cell infiltration predominantly into VAT

Received: 28 June 2023. **Editorial Decision:** 9 September 2023. **Corrected and Typeset:** 27 September 2023

may define subphenotypes of insulin-resistant cardiometabolically high-risk obesity (6).

AT inflammation in obesity engages T and B lymphocytes, natural killer and NK T cells, macrophages, monocytes, dendritic cells, neutrophils, and mast cells, which change in their relative tissue abundance and exhibit altered polarization state(s) (7-10). This frequently considered chronic, low-grade "sterile" inflammatory change of the tissue also involves dysregulated expression and secretion of metabolites and proinflammatory cytokines and chemokines, of which tumor necrosis α (TNFα), interleukin 6 (IL6), and CCL2 (MCP-1) are considered prototypic (7, 11). The exact evolution of AT inflammation in obesity is not fully understood but is consistent with the concept that inflammation has a wide spectrum that involves perturbed homeostatic regulation, tissue dysfunction, and structural tissue changes (such as fibrosis and accumulation of senescent cells) (12). Overall, since the degree of VAT inflammation seems to correlate with the risk of obesity-associated cardiometabolic complications (4, 13), estimating VAT inflammation can assist in obesity subphenotyping and cardiometabolic risk stratification.

A major limitation in assessing VAT inflammation is the inaccessibility of this fat depot for sampling in nonsurgical patients. This highlights the need for clinically available alternatives that use biomarker surrogates to determine VAT inflammation. So far, there is no circulating biomarker that reflects the extent of VAT inflammation. In the present study, we therefore focused on circulating microRNAs (circ-miRs) in relation to the inflammation state in VAT. miRNAs are short (17-25 nucleotides), noncoding RNA molecules that function as negative regulators of gene expression by 2 main processes that rely on sequence recognition of target messenger RNAs (mRNAs): mRNA destabilization, and translational inhibition (14). Although miRNAs function intracellularly, they are also found in the circulation, either unbound, within extracellular vesicles, or bound to high-density lipoproteins (HDLs) (15-17). They are increasingly considered as reliable biomarker molecules, partially because of their relative stability in plasma samples and the availability of various procedures to detect them. Adipose tissue, particularly in obesity, is a major source of circ-miRs, with an estimated contribution of up to 50% of all circ-miRs (based on mouse models of obesity(18)).

In the present study, we hypothesized that circ-miRs reflect the extent of VAT inflammation defined by proinflammatory gene expression signatures. Using a "discovery cohort," we identified putative circ-miRs with discriminative power between patients with obesity with either low or high VAT inflammation, and used stringent bioinformatic tools to predict whether they may also contribute functionally to obesity-related complications. Since miRNA studies typically suffer from poor reproducibility between different cohorts (19, 20), we validated our results in an independent cohort. Jointly, we propose a circ-miR–based approach to discriminate between patients with obesity and either low or high VAT inflammation phenotypes, in the quest to better personalize obesity management.

Materials and Methods

Study Participants

Both the discovery (n = 35) and the validation (n = 51) cohorts were assembled from an ongoing recruitment program supporting an adipose tissue biobank, as previously reported (21). Patients undergoing elective abdominal surgery at Soroka University Medical Center gave written informed consent for depositing blood and VAT (omental) samples into the biobank. For the present study, patients who met the eligibility criteria, underwent bariatric surgery, were aged 18 to 70 years, had a body mass index (BMI) of 30 or greater, and had no known malignancies, were included. Soroka University Medical Center's ethical review board approved the study in advance (approval No. 0348-15-SOR).

Clinical and Biochemical Assessment

All study participants were hospitalized one day before the scheduled operation. On admission, they were clinically evaluated according to the currently accepted guidelines (22), including vital signs and anthropometric indices measurements. Following overnight fasting, the morning of the operation, an extended biochemical workup was conducted. This included complete blood count, blood chemistry (glucose and electrolytes, kidney and liver function, full lipogram and glycated hemoglobin A_{1c}), C-reactive protein, and endocrine evaluation including insulin. A blood sample for future analysis of circ-miRs was drawn on the same occasion. We further calculated the homeostatic model assessment of insulin resistance (HOMA-IR), triglycerides to HDL ratio, and triglycerides to glucose index (23). To diminish the degree of hemolysis we used a 21-gauge needle and strictly followed the recommendations on blood sample collection (24).

Estimation of Visceral Adipose Tissue Inflammation

RNA was extracted from VAT by RNeasy Lipid Tissue Mini Kit (Qiagen, catalog No. 74804). Complementary DNA (cDNA) was created using High-Capacity cDNA Reverse Transcription Kit (Applied Biosystems catalog No. 4368814). Expression of *TNFA*, *IL6*, and *CCL2* was measured using TaqMan gene expression assays by quantitative polymerase chain reaction (qPCR) (ThermoFisher catalog Nos. Hs00174128, Hs00234140, and Hs00174131, respectively). Endogenous control genes *PPIA* and *PGK1* (ThermoFisher catalog Nos. Hs99999904 and Hs99999906, respectively) were used to control for technical variance (25). VAT inflammation score was created by dividing the expression of each inflammatory gene into tertiles, and each tertile was given an intermediate score of 0 to 2 from lower to higher. The intermediate score for each gene was summarized to generate a VAT inflammation score of 0 to 6. Patients with scores 0 to 2 were considered to have low-VAT inflammation, while patients with scores 4 to 6 were considered as high-VAT inflammation. Patients with a VAT inflammation score of 3 were excluded from the group analyses (n = 5 and 10 in the discovery and validation cohorts, respectively) to reduce misclassification bias (Supplementary Table S1 (26)).

Clinical Assessment of Visceral Adipose Tissue Inflammation

We estimated the degree of VAT inflammation using demographic (eg, age, sex), clinical (eg, dysglycemia, hypertension), and commonly available biochemical (eg, fasting glucose, triglycerides, HDL cholesterol) data, as well as insulin and HOMA-IR (Table 1). These data were evaluated by 2 independent endocrinologists (L.B. and U.Y.) blinded to the

Table. 1. Patient characteristics and biochemical parameters

Clinical parameters	Discovery cohort						Validation cohort						Entire cohort comparison, *P*
	Entire cohort n = 35		VAT inflammation (score)				Entire cohort n = 51		VAT inflammation (score)				
			low (0-2); n = 16		high (4-6); n = 14	*P*			low (0-2); n = 21		high (4-6); n = 20	*P*	
	median	IQR	median	IQR	median	IQR		median	IQR	median	IQR	median	IQR		
Age, y	43 ± 18		39 ± 20		43 ± 15	.30	42 ± 27		40 ± 30		46 ± 22	.69	.65
Sex (% female/total)	83% (29/35)		81% (13/16)		86% (12/14)	.74	80% (41/51)		90% (19/21)		65% (13/20)	.05	.77
BMI	40 ± 8		40 ± 7		42 ± 10	.16	43 ± 11		43 ± 15		42 ± 7	.54	.39
First bariatric surgery (%)	60% (21/35)		56% (9/16)		64% (9/14)	.65	53% (27/51)		52% (11/21)		55% (11/20)	.87	.52
Diastolic BP, mm Hg	80 ± 26		77 ± 23		80 ± 29	.65	75 ± 13		75 ± 14		74 ± 15	.74	.89
Systolic BP, mm Hg	128 ± 18		131 ± 25		128 ± 9	≥.999	130 ± 21		129 ± 22		130 ± 20	.73	.81
TGs, mg/dL	143 ± 148		148 ± 118		127 ± 127	.37	124 ± 96		108 ± 54		150 ± 103	.06	.73
LDL, mg/dL	97 ± 30		100 ± 27		92 ± 48	.05	91 ± 34		89 ± 33		97 ± 38	.57	.18
HDL, mg/dL	44 ± 14		49 ± 18		42 ± 10	.20	41 ± 12		43 ± 9		40 ± 14	.32	.50
TGs/HDL ratio	2.6 ± 3.9		3.4 ± 3.7		2.8 ± 3.5	.71	3.1 ± 2.4		2.6 ± 1.9		3.4 ± 3.8	.09	≥.999
TGs/FPG ratio	1.31 ± 1.02		1.59 ± 1.20		1.21 ± .80	.24	1.40 ± 0.85		1.10 ± 0.70		1.45 ± 0.85	.12	≥.999
FPG, mg/dL	96 ± 25		94 ± 14		97 ± 26	.26	93 ± 20		93 ± 22		96 ± 23	.67	.37
HbA_{1c}, %	5.5 ± 0.5		5.6 ± 0.6		5.5 ± 0.4	.95	5.7 ± 0.6		5.7 ± 0.5		5.6 ± 0.7	.90	.72
Insulin, µU/mL	15.4 ± 11.7		12.0 ± 13.1		18.8 ± 8.2	.12	10.8 ± 10.9		11.4 ± 12.8		10.0 ± 6.3	.15	.31
HOMA-IR, AU	4.05 ± 2.98		2.80 ± 3.23		4.61 ± 1.62	.12	2.50 ± 2.70		2.55 ± 2.68		2.35 ± 1.35	.40	.27
Prediabetic (%)	20% (7/35)		25% (4/16)		14% (2/14)	.46	22% (11/51)		24% (5/21)		30% (6/20)	.66	.86
Diabetes (%)	20% (7/35)		12% (2/16)		29% (4/14)	.27	14% (7/51)		14% (3/21)		15% (3/20)	.95	.44
MS (%)	60% (21/35)		56% (9/16)		71% (10/14)	.39	73% (37/51)		67% (14/21)		75% (15/20)	.56	.22
No. of MS parameters	3.0 ± 2.0		3.0 ± 2.3		3.0 ± 1.5	.80	3.0 ± 2.0		3.0 ± 1.0		3.5 ± 1.3	.22	.35
SGOT, U/L	22 ± 13		22 ± 16		20 ± 11	.45	20 ± 5		21 ± 6		20 ± 5	.46	.05
SGPT, U/L	21 ± 14		21 ± 13		23 ± 11	.33	18 ± 12		19 ± 11		17 ± 11	.57	.14
CRP, mg/dL	1.06 ± 1.24		0.96 ± 0.92		1.14 ± 1.03	.45	0.78 ± 0.99		0.78 ± 1.54		0.76 ± 0.78	.33	.18

Data are shown for the entire discovery (n = 35) and validation (n = 51) cohorts in the left column for each cohort. Also shown is a comparison between the low-VAT inflammation group (score 0-2) and the high-VAT inflammation group (score 4-6). The *P* values are computed by Mann-Whitney test for continuous data and chi-square test for categorical data.
Abbreviations: AU, arbitrary units; BMI, body mass index; BP, blood pressure; CRP, C-reactive protein; FPG, fasting plasma glucose; HbA_{1c}, glycated hemoglobin A_{1c}; HDL, high-density lipoprotein; HOMA-IR, homeostatic model assessment of insulin resistance; IQR, interquartile range; LDL, low-density lipoprotein; MS, metabolic syndrome; SGOT, glutamate oxaloacetate transaminase; SGPT, glutamate pyruvate transaminase; TGs, triglycerides; VAT, visceral adipose tissue.

laboratory-derived inflammation score, with the aim of clinically classifying the degree of VAT inflammation as being high or low. In cases of disagreement, the decision was made by a third evaluation by an experienced diabetologist, who was blinded to the inflammation score as well (I.F.L.). As universal guidelines for clinical assessment of the degree of VAT inflammation are lacking, the evaluating physicians were instructed to follow their routine practice in the metabolic clinic, using their clinical skills and experience. The final clinical decision was then compared against the molecular evaluation by the VAT inflammation score, which served as the reference standard.

Analysis of Circulating MicroRNA

MicroRNA extraction

miRNAs were extracted from plasma samples with the use of the miRNeasy Plasma Advanced Kit (Qiagen, catalog No. 217204). As a technical control for miRNA recovery, *C elegans* miRNA Cel-miR-39 (UCACCGGGUGUAAAUC AGCUUG, Thermo custom order) was added at 5 pg/sample (phosphate was added to the 5-prime of the sequence for compatibility with TaqMan assays). Hemolysis was evaluated using qPCR to avoid contamination with miRNAs known to be prevalent in erythrocytes. We assessed the levels of miR-451a and miR-23a-3p, which correspond to the contributions of red blood cells (RBCs) and plasma, respectively (Thermo Fisher, AB-A25576-478107_mir and AB-A25576-478532_mir). Samples were considered nonhemolytic and adequate for further analysis when (CT miR-23a-3p) – (CT miR-451a) was less than 7 (27).

Libraries construction in the discovery cohort

Following the determination of 35 samples as being eligible, libraries were created using the QIAseq miRNA Library Kit (Qiagen, catalog No. 331505). Initially, cDNA was generated and then purified using magnetic beads provided in the kit. Subsequently, the libraries were amplified and subjected to an additional purification step. Finally, next-generation sequencing (NGS) was conducted using NextSeq 500/550 High-Output Kit v2.5 (75 Cycles, catalog No. 20024906).

Bioinformatic analysis

The adapters in the FASTQ files were removed using Cutadapt (28) with the following command: "cutadapt -a AACTGTAGGCACCATCAAT -m 17." The quality of the cleaned files was then assessed using FastQC (http://www.bioinformatics.babraham.ac.uk/projects/fastqc). To quantify the levels of small RNA in the samples, miRGE3 (29) was employed. Using the RPM (reads per million) file generated by miRGE3, the average and maximum abundance of each miRNA across all libraries were calculated. miRNAs that met the criteria of having an average count greater than 5 RPM and a maximum count greater than 50 RPM, and were present in all libraries, were considered for further analysis.

To identify differentially expressed miRNAs (DEMs) between patients with high- and low-VAT inflammation, we used Mann-Whitney test and Deseq2 (30) (with R). For both analyses, a miRNA was considered statistically significantly different if the *P* value was .05 or less. To evaluate the miRNAs' potential to distinguish between patients with high-/low-VAT inflammation, the expression levels of miRNAs were subjected to receiver operating characteristic (ROC) analysis. Discriminative miRNAs were indicated by ROC-AUC (area under the curve) values of 0.8 or greater and with the lower CI values being greater than 0.5. Circ-miRs that were identified in the discovery cohort by all 3 statistical approaches were considered putative VAT inflammation-associated circ-miRs (VIA-circ-miRs).

Quantitative polymerase chain reaction analysis of circulating microRNAs in the validation cohort

As there is no gold standard for adjusting circ-miRs levels to compare between different samples (31), we used the abundance of circ-miRs 23a-3p, 361-5p, and 191-5p (ThermoFisher catalog Nos. AB-A25576-478532_mir, AB-A25576-478056_mir and AB-A25576- 477952_mir) as endogenous control circ-miRs. This was based on their abundance level that corresponded to those of our putative VIA-circ-miRs (mean abundance was RPM > 50), and because they exhibited the lowest coefficient of variation among all circ-miRs between participants of the discovery cohort. Expression levels of the putative VIA-circ-miRs 181b-5p, 1306-3p, 3138 and 423-5p (Thermo Fisher catalog Nos. AB-A25576- 478583_mir, AB-A25576-479575_mir, AB-A25576- 479624_mir, and AB-A25576-478090_mir) were measured by qPCR and calculated relative to the mean of the 3 control miRs.

Visceral adipose tissue inflammation–associated circulating microRNA sensitivity to hemolysis

To test the sensitivity of putative VIA-circ-miRs to hemolysis, we generated "pseudo-hemolytic" samples by adding RBC lysate to low-hemolytic plasma, as previously described (32). For this, RBCs were isolated from a single blood sample after centrifugation and were lysed mechanically. Final added RBC lysate concentration in the plasma (by serial dilutions) was 0.0005% to 0.001% (v/v) for "low RBC lysate" and 0.125% to 0.25% (v/v) for "high RBC lysate." Levels of putative VIA-circ-miRs were measured by qPCR, as described earlier.

KEGG pathway analysis

Target genes of miR-181b-5p, 1306-3p, and 3138 were predicted using Targetscan v8 (https://www.targetscan.org/vert_80/). The list of predicted targets was uploaded to the Database for Annotation, Visualization and Integrated Discovery (DAVID) (https://david.ncifcrf.gov/tools.jsp). Using the functional annotation tool, we obtained the list of enriched KEGG pathways, from which we focused on those that are relevant to metabolism, cell signaling, and inflammation.

Additional graphical and statistical analyses. Graphical software and statistical analyses beyond those already mentioned (using R) were performed with GraphPad Prism (version 9).

Results

Discovery and Validation Cohorts With Low- vs High-Visceral Adipose Tissue Inflammation

The workflow of this biomarker discovery study is presented in Fig. 1A. A discovery cohort and an independent validation cohort were assembled by selecting consecutive n = 35 and

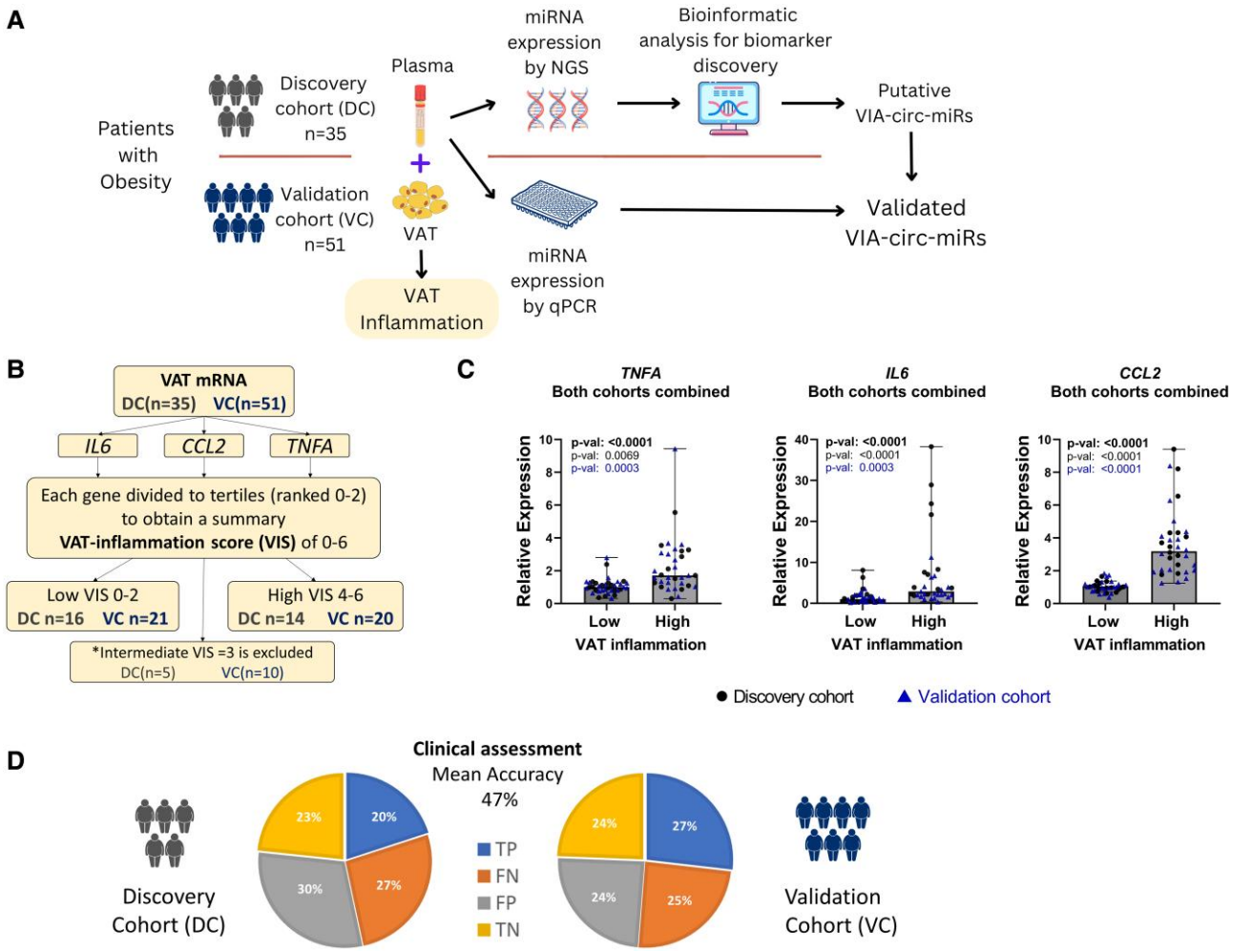

Figure 1. Overview of study design and rationale. Discovery cohort (n = 35) and validation cohort (n = 51) of patients living with obesity were included in this study. A, Study overview: In both the discovery and the validation cohorts, VAT samples were taken for evaluation of VAT inflammation (explained in B). Blood was drawn for biochemical parameters, and miRNAs were extracted from plasma. In the discovery cohort miRNAs were sequenced by next-generation sequencing (NGS). Bioinformatic analysis was performed to identify all miRNAs above an abundance threshold that showed differential expression in the "high VAT inflammation" group (= putative VIA-circ-miRs). Validation of VIA-circ-miRs was performed by quantitative PCR. B, VAT inflammation was assessed using the mRNA expression levels of *TNF*, *IL6*, and *CCL2*. Each gene expression was divided into tertiles and given a score of 0 to 2. The score was summarized for all 3 genes to generate a total VAT inflammation score of 0 to 6. Participants were divided into 2 groups according to the VAT inflammation score: "low": 0 to 2, and "high": 4 to 6. A group of patients with an intermediate VAT inflammation score of 3 was excluded to lower the risk of misclassification bias. C, mRNA expression levels of *TNFA*, *IL6*, and *CCL2* in VAT of participants in the discovery cohort (black symbols) and validation cohort (blue symbols), relative to endogenous control genes (*PPIA* and *PGK1*) determined by quantitative real-time polymerase chain reaction. Compared are those with low (score 0-2, n = 16 and n = 21 in the discovery and validation cohorts, respectively) or high (score 4-6, n = 14 and n = 20 in the discovery and validation cohorts, respectively) VAT inflammation score. *P* values were computed with the Mann-Whitney test. *P* values shown in black, blue, and black-bold are for the discovery cohort, validation cohort, and combined cohorts, respectively. D, Estimation of VAT inflammation by physicians based on patients' clinical characteristics only. A pie chart showing the performance of the clinical evaluation compared to the lab-based evaluation of VAT inflammation in both cohorts. FN, false negative; FP, false positive; mRNA, messenger RNA, miRNA, microRNA; TN, true negative; TP, true positive; VAT, visceral adipose tissue.

n = 51 patients, respectively, who are living with obesity and were recruited to our human adipose tissue biobank. In both cohorts, participants were scored according to a "VAT inflammation score" based on the relative mRNA expression of 3 prototypic inflammatory genes, *TNFA*, *IL6*, and *CCL2* (Fig. 1B): We summed the tertile level of expression (graded 0-2) of each of the 3 genes, resulting in a score range of 0 to 6. To minimize misclassification bias, when conducting a between-group comparison of low- vs high-VAT inflammation, we excluded 5 and 10 participants in the discovery and validation cohorts, respectively, whose VAT inflammation score was "intermediate"—that is, who received a value of 3. Yet, for correlation analyses (discussed later), all n = 86 participants were included in the analysis. In both cohorts separately, and when joined, each of the 3 genes composing the VAT inflammation score was significantly elevated among the high- (compared to the low-) VAT inflammation subgroup (Fig. 1C). Moreover, among participants of both cohorts, *CCL2* significantly ($P < .001$) intercorrelated with the expression of both *TNFA* and *IL6*, which in turn did not intercorrelate between themselves. Yet, even the significant correlations did not reach colinearity (coefficient of correlation <0.6), and the expression of neither of the individual genes fully separated, on its own, those with high- vs low-VAT inflammation. We reasoned this suggests that each gene can contribute a distinct, nonredundant aspect of VAT inflammatory status that is better represented by the joint expression level of the 3 prototypic proinflammatory genes.

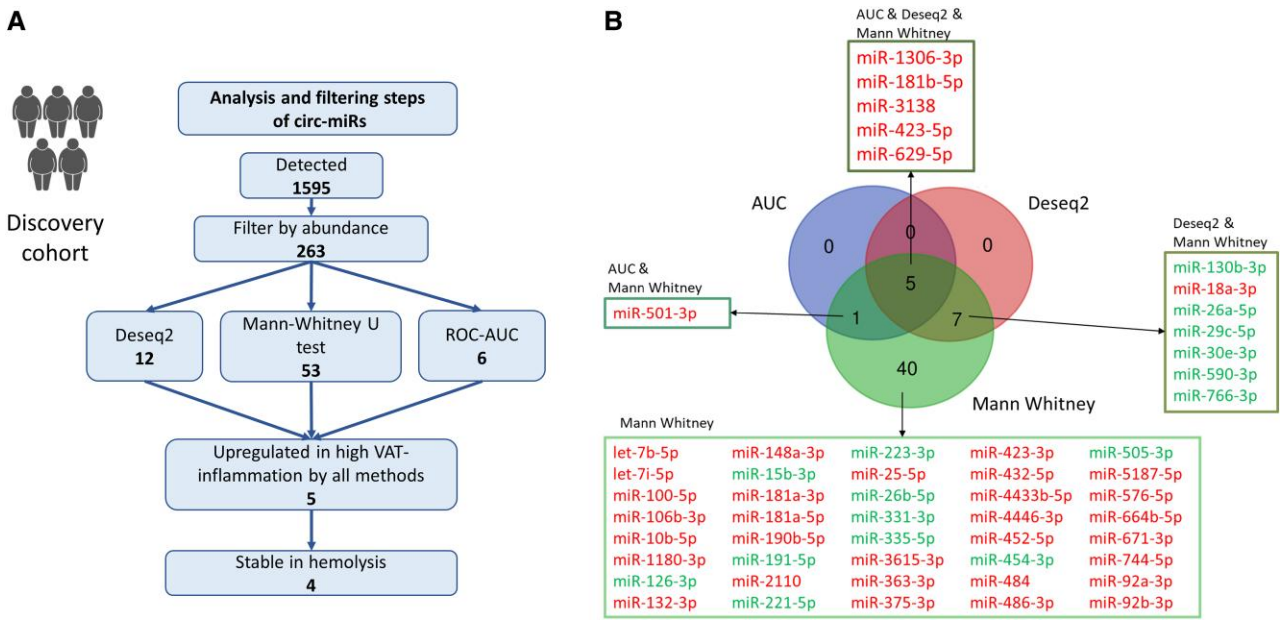

Figure 2. Identifying putative VIA-circ-miRs. A, Steps performed to identify putative VIA-circ-miRs in the discovery cohort: circ-miRs were filtered by abundance across all libraries (minimal RPM > 0, average RPM > 5, maximal RPM > 50); differential expression by Mann-Whitney *U* test and by Deseq2 ($P<.05$); discriminative power by ROC-AUC (ROC-AUC≥0.8). B, Venn diagram showing differentially abundant circ-miRs according to 3 independent statistical approaches. miRNAs that are more or less abundant in high vs low VAT inflammation subgroups are marked in red and green, respectively. AUC, area under the curve; miRNA, microRNA; ROC, receiver operating characteristic; RPM, reads per million; VAT, visceral adipose tissue; VIA-circ-miRs, VAT inflammation-associated circ-miRs.

The clinical characteristics of the 2 complete cohorts, and their group division into those with low- (score 0-2, n = 16 and n = 21 in the discovery and validation cohort, respectively) and high- (score 4-6, n = 14 and n = 20, respectively) VAT inflammation is presented in Table 1. There were no statistically significant differences between the cohorts—or within each cohort—between the 2 subgroups, in any individual parameter, indicating that patients were not overtly clinically/phenotypically distinct. In the discovery cohort (but not in the validation cohort), those with high VAT inflammation scores trended to be more insulin resistant, based on HOMA-IR, compared to those with low VAT inflammation scores.

We first determined if the VAT inflammation status, established by VAT gene expression-based score, could be predicted by clinicians blinded to the score, based only on the clinical parameters of the patients (as detailed in "Materials and Methods"). Despite very high inter-rater agreement (90% and 85% in the discovery and validation cohort, respectively), the ability to clinically estimate VAT inflammatory status against the gene expression–based score was low (Fig. 1D), with true positive rates of 0.429 and 0.524, and accuracy of 0.433 and 0.512, in the discovery and validation cohorts, respectively. This performance underscores the currently unmet need to find biomarkers that could aid in subphenotyping/risk-stratifying patients with obesity based on their VAT inflammatory state, even when it is relatively subtle/early and without/before overt clinical manifestations.

Identifying Circulating MicroRNAs Indicative of Visceral Adipose Tissue Inflammation

We used plasma samples of the discovery cohort to identify candidate VIA-circ-miRs. We ensured that plasma miRNA recovery was technically comparable by spiking-in *C elegans* miRNA and measuring its abundance after extraction. In addition, to rule out different contribution of miRNAs from RBCs, we confirmed low levels of hemolysis, as detailed in "Materials and Methods." miRNA libraries were constructed and sequenced by NGS. Out of the 1595 identified circ-miRs, 263 passed an abundance threshold of minimal RPM greater than 0 in all libraries, average of 5 or greater, and maximum of 50 or greater (Fig. 2A).

To detect putative VIA-circ-miRs, we performed 3 types of statistical analyses for defining those miRNAs that differ significantly between participants in the discovery cohort, whose obesity was accompanied by a low vs high VAT inflammation score. Mann-Whitney resulted in 53 DEMs, Deseq2 analysis resulted in 12 DEMs, and discriminative power ROC-AUC analysis resulted in 6 miRNAs. Five of the DEMs were common between all 3 statistical approaches (Fig. 2B), all with upregulated expression in the high-VAT inflammation group (Fig. 3A). Since levels of some circ-miRs may be highly sensitive to hemolysis given their relatively high abundance within RBCs, we assessed this for the 5 putative VIA-circ-miRs as follows. We generated test samples representing either very low or high hemolysis (ie, ~0 or 0.25% hemolysate of RBC, respectively). Of the 5 putative VIA-circ-miRs, the abundance of circ-miR-629-5p was significantly higher in samples representing high vs low hemolysis (Fig. 3B). We therefore excluded circ-miR-629-5p from further analysis.

Since a key characteristic of a useful biomarker is its robustness and reproducibility, we next wished to validate the 4 remaining putative VIA-circ-miRs seen in the discovery cohort in an independent cohort (Fig. 3C), and using a methodology different from the NGS used for VIA-circ-miRs discovery. In samples of the validation cohort, we assessed VAT inflammation, and extracted plasma miRNAs, exactly as in the discovery cohort, and the abundance of the 4 putative VIA-circ-miRs was measured by PCR. Circ-miRs 181b-5p, 1306-3p, and 3138 levels were significantly, or nearly so, higher in participants of the validation cohort with high VAT inflammation

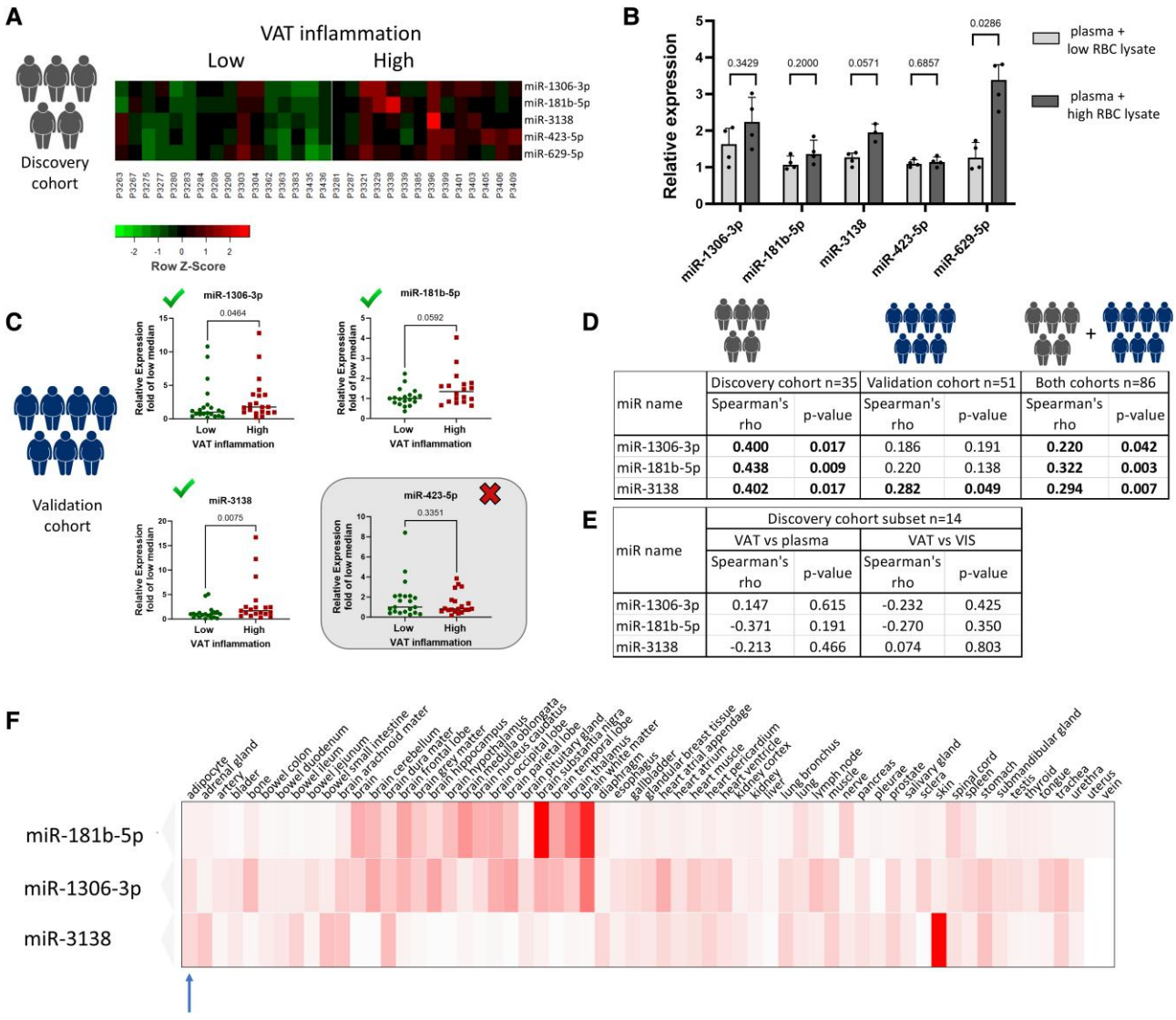

miR name	Discovery cohort n=35		Validation cohort n=51		Both cohorts n=86	
	Spearman's rho	p-value	Spearman's rho	p-value	Spearman's rho	p-value
miR-1306-3p	**0.400**	**0.017**	0.186	0.191	**0.220**	**0.042**
miR-181b-5p	**0.438**	**0.009**	0.220	0.138	**0.322**	**0.003**
miR-3138	**0.402**	**0.017**	**0.282**	**0.049**	**0.294**	**0.007**

miR name	Discovery cohort subset n=14			
	VAT vs plasma		VAT vs VIS	
	Spearman's rho	p-value	Spearman's rho	p-value
miR-1306-3p	0.147	0.615	-0.232	0.425
miR-181b-5p	-0.371	0.191	-0.270	0.350
miR-3138	-0.213	0.466	0.074	0.803

Figure 3. Validation of putative VIA-circ-miRs. A, A heat map showing the expression *z* scores of identified circ-miRs in each participant in the discovery cohort divided to low- and high-VAT inflammation subgroups. B, Relative abundance of the 5 putative VIA-circ-miRs in plasma samples to which low (0.0005-0.001% v/v) vs high (0.125-0.25% v/v) RBC lysate was added. *P* values were computed with the Mann-Whitney test. C, Quantitative rt-PCR results of plasma expression of 4 putative VIA-circ-miRNAs that passed the hemolysis test, comparing patients with low- vs high-VAT inflammation in the validation cohort. *P* values were computed with the Mann-Whitney test. miRNAs that passed the significance threshold ($P < .05$) or came close are marked with green check marks. D, Spearman correlations of the 3 validated VIA-circ-miRs with VAT inflammation score for the discovery cohort (n = 35), validation cohort (n = 51), and both cohorts combined (n = 86). Bold font indicates statistically significant correlations. E, Spearman correlations between expression of the 3 validated VIA-circ-miRs in VAT and their abundance in plasma and VAT inflammation score (VIS) for a subset of the discovery cohort (n = 14). F, The normalized expression of the 3 VIA-circ-miRNAs in different tissues according to TissueAtlas database. The arrow points to "adipocyte." miRNA, microRNA; VAT, visceral adipose tissue; VIA-circ-miRs, VAT inflammation-associated circ-miRs; VIS, VAT inflammation score.

(see Fig. 3C). Conversely, the higher abundance of circ-miR-423-5p observed in the discovery cohort (see Fig. 3A) could not be validated (see Fig. 3C). We therefore continued the validation process for the remaining 3 circ-miRs, using correlation analysis, complementing the 2-subgroup comparison (Fig. 3D). This approach enabled us to include also the 5 and 10 participants in the discovery and validation cohorts, respectively, whose VAT inflammation score was intermediate and were excluded from the initial subgroup comparison. The Spearman correlation coefficient was positive for all 3 circ-miRs in both cohorts, but did not reach statistical significance for circ-miR-181 and 1306-3p in the validation cohort alone. Nevertheless, when expressing the abundance level in the 2 cohorts as fold-of-mean and combining the data (n = 86), all 3 circ-miRs positively correlated with VAT inflammation score ($P \leq .05$) (see Fig. 3D). We questioned whether VAT may be a source of these miRNAs using a subanalysis of n = 14 participants of the discovery cohort, for whom we measured VAT expression of miRNAs. To this end, neither of the miRNAs significantly correlated in their abundance in the circulation (plasma) with expression level in VAT, and their expression level in VAT did not correlate with VAT inflammation score (Fig. 3E). Moreover, tissue expression information obtained from TissueAtlas (33) suggested that adipocytes are not among the most highly expressing cell type of any of the 3 miRNAs (Fig. 3F). Though not conclusive, these analyses do not provide strong support for VAT as a major contributor for the circulating abundance of the 3 miRNAs. Collectively, we identified 3 VIA-circ-miRs validated in 2 independent cohorts of patients with obesity.

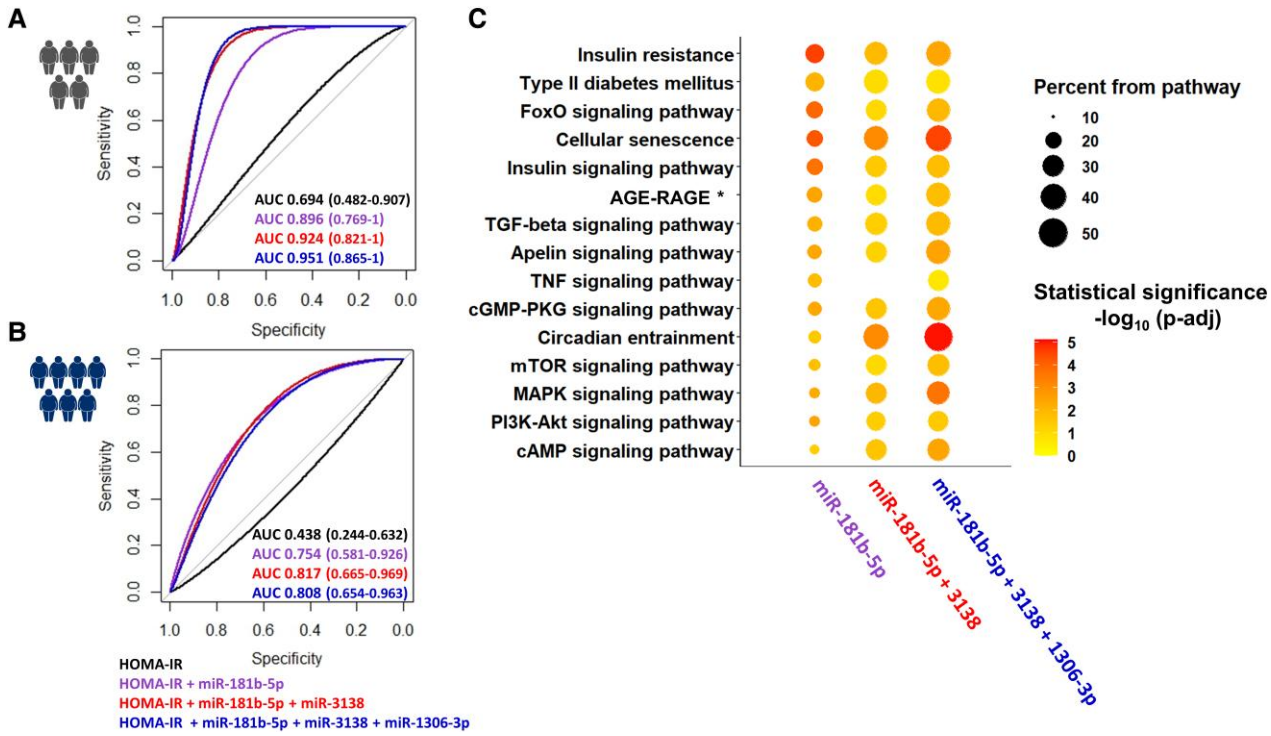

Figure 4. Discriminative power of the VIA-circ-miRs and target pathway enrichment analysis. Discriminative power of HOMA-IR alone and sequential combination with validated VIA-circ-miRs in A, discovery cohort (n = 30). B, Validation cohort (n = 41) that includes participants with low- and high-VAT inflammation. C, KEGG pathways analysis of the predicted targets for gradually combined circ-miRs 181b-5p, 1306-3p, and 3138. *AGE-RAGE signaling pathway in diabetic complications. *P* value adjusted for multiple testing (*P*adj) was computed by the Functional Annotation tool in DAVID (43). HOMA-IR, homeostatic model assessment of insulin resistance; miRNA, microRNA; VAT, visceral adipose tissue; VIA-circ-miRs, VAT inflammation-associated circ-miRs.

Using Validated Visceral Adipose Tissue Inflammation–Associated Circulating MicroRNA to Discriminate Between Patients With Obesity and High- vs Low-Visceral Adipose Tissue Inflammation

ROC analyses were used to determine the ability of the 3 validated VIA-circ-miRs, alone or in combination with other VIA-circ-miRs and/or clinical characteristics, to discriminate between patients with obesity and high- vs low-VAT inflammation. The results of all possible combinations of VIA-circ-miRs with various single clinical parameters are provided in Supplementary Table S2 (26). Since VAT inflammation is strongly implicated in the development of systemic insulin resistance, we assessed the ability to improve the discriminative power of this parameter using validated VIA-circ-miRs. HOMA-IR as a single parameter poorly discriminated between the 2 subgroups, with an ROC-AUC of 0.694 and 0.438 for the discovery and validation cohorts, respectively (Fig. 4A and 4B). The combination of HOMA-IR and circ-miR-181b-5p (a miRNA well documented to be associated with inflammation) markedly increased the discriminative power, reaching 0.896 and 0.754 in the discovery and validation cohorts, respectively. The addition of circ-miR 3138 added discriminative power in both cohorts, whereas the final addition of miR 1306-3p only minimally changed the ROC-AUC value of the combined model for both cohorts. Nevertheless, HOMA-IR in combination with circ-miRs 181b-5p, 1306-3p, and 3138 exhibited highly discriminative ability (considered as ROC-AUC > 0.8) between patients with high- or low-VAT inflammation (see Fig. 4A and 4B).

Pathways Putatively Targeted by Visceral Adipose Tissue Inflammation–Associated Circulating MicroRNAs

Some support for the biological plausibility of our findings could be provided by pathway enrichment analysis of predicted targets of miRNA-181b-5p alone, miRNAs 181b-5p + 3138, and miRNAs 181b-5p + 3138 + 1306-3p. Interestingly, predicted targets of miRNA-181b-5p were enriched in pathways highly relevant to obesity complicated by high-VAT inflammation, including the TNF signaling pathway, insulin signaling, insulin resistance, and type 2 diabetes (Fig. 4C). Cellular senescence and circadian entrainment pathways were also intriguingly significantly enriched among targets of miRNA-181b-5p. When adding the 2 other validated VIA-circ-miRs sequentially, many of these significantly enriched pathways either involved a larger number of genes and/or such enrichment became more statistically significant. For example, the insulin resistance pathway involved 26 genes (24%) that are miRNA-181b-5p targets, and 40 genes (37% of the pathway) when considering putative targets of all 3 VIA-circ-miRs. Circadian entrainment, cellular senescence, and mitogen-activated protein kinase signaling all exhibited, in addition to an increase in the percentage of genes of the pathways, a greater significance of the enrichment when considering the 3 VIA-circ-miRs vs miRNA-181b-5p alone (see Fig. 4C). This analysis may suggest that the 3 miRNAs overlap in their biological activity, consistent with the modest change in discriminative capacity when combining all 3 to distinguish between patients with obesity and high- vs low-VAT inflammation.

Discussion

In this study, we used a biomarker discovery approach for testing the hypothesis that distinct circ-miRs could constitute biomarkers of VAT inflammation in obesity. The motivation for this study is the currently unmet clinical need to subphenotype/risk-stratify patients living with obesity given its high and still increasing prevalence. VAT inflammation is linked, mainly by cross-sectional studies, but also by prospective studies, with poorer health end points in obesity (34), but unlike SAT, VAT is not amenable for sampling in nonsurgical patients. Our results demonstrate that adding circ-miRs to HOMA-IR measurement greatly improves the ability to identify patients with high- vs low-VAT inflammation, even when VAT inflammation–related characteristics are not clinically overt. Using a discovery and an independent validation cohort paradigm, and 2 distinct laboratory methodologies to measure the circulating levels of putative VIA-circ-miRs, these results can assist in subphenotyping patients living with obesity beyond currently available clinical tools, hence potentially contributing to personalizing obesity management.

The biological plausibility for linking at least 2 of the 3 VIA-circ-miRs (circ-miRs 181b-5p, 1306-3p, 3138) to VAT inflammation in obesity is supported by pathway enrichment analysis of their targets, and by existing literature. Of the 3, miR-181b-5p has been the most reported to be linked to the pathophysiology of obesity and its complications. Upregulation of this miRNA attenuated vascular nuclear factor-κB–mediated inflammation (35), and improved AT vascular response to insulin by targeting a protein kinase B phosphatase (36). AT expression of miR-181b-5p was reported to be downregulated in obesity (36), a trend we also observed in a small subset of our participants (though nonsignificantly; see Fig. 3E). This suggests that either AT is not the likely source of elevated circ-miR-181b-5p, or conversely, that enhanced secretion of this miRNA from AT results in elevated circulating levels but decreased AT abundance, which in turn contributes to VAT inflammation. Intriguingly, in the liver, miR-181b-5p targets Sirt1 and contributes to nonalcoholic fatty liver disease (37). Thus, an intriguing speculation that is worth further investigation is that increased release of miRNA 181b-5p from AT mediates a pathogenic fat-liver communication in obesity with high-VAT inflammation.

There are rather sparse data on the 2 other VIA-circ-miRs (circ-miRs 3138 and 1306-3p). miRNA 3138 has been shown in human umbilical vein endothelial cells to be upregulated by chronic hyperinsulin conditions and target kinase suppressor of ras 2, thereby affecting reactive oxygen species generation, insulin signaling, and energy metabolism (38). Nevertheless, a direct link with inflammation has not been reported. Similarly, miRNA 1306-3p has mainly been reported in the context of gastrointestinal cancers (39, 40), and recently in the pathogenesis of visceral pain (41), but not related to inflammation or metabolic or endocrine diseases. Suggestive from our targets' pathway enrichment analysis, the 2 miRNAs may target additional genes that function within pathways targeted by miR-181b-5p, including, interestingly, circadian entrainment and cellular senescence. These 2 pathways most evidently engage a larger percentage of the genes constituting the pathway, and with higher statistical significance, when adding predicted targets of miR-3138 and miR-1306-3p. Jointly, these analyses and the published literature support our unbiased discovery approach, providing putative mechanisms for the link with VAT inflammation in obesity that requires independent investigations to be proven.

Our study has several specific strengths and limitations worth mentioning. We have a modest number of participants from a single-center biobank. Yet, acknowledging concerns about the reproducibility of miRNA-related studies (42), we validated our findings from a discovery cohort in an independent validation cohort. Also, we have directly assessed VAT inflammation by measuring the expression of prototypic inflammatory genes in the VAT itself. It is noteworthy that the clinical characteristics of the 2 cohorts were not identical. In both cohorts, the subgroup with high VAT inflammation did not significantly differ in any single parameter from the subgroup with low VAT inflammation, consistent with the poor performance of clinically based estimates of VAT inflammatory status. Yet, although only in the discovery cohort, we observed trends for worse metabolic phenotypes associated with high-VAT inflammation. Since our validation procedure was a prerequisite for moving from "putative" to "validated" VIA-circ-miRs, these biomarkers do not depend on, and their abundance may precede, overt clinical manifestations of VAT inflammation. Importantly, we used different methods to measure circ-miRs —i.e., NGS in the discovery cohort, and real-time PCR in the validation cohort—ensuring that the validated VIA-circ-miRs can be measured by a readily available laboratory technique. Finally, this study is limited in being a cross-sectional analysis, so the ability to predict future clinical end points using VIA-circ-miR–based tools awaits additional studies.

In summary, circ-miRs 181b-5p, possibly with 1306-3p and/or 3138, can form a basis for the development of a clinical calculator to effectively assess VAT inflammation in obesity, constituting a "liquid-biopsy-like" strategy to better personalize obesity care.

Acknowledgments

Special thanks to Alon Zemer for critically reviewing the manuscript.

Funding

This work was supported by the Deutsche Forschungsgem einschaft (DFG, German Research Foundation grant No. 209933838: SFB1052: "Obesity mechanisms") and the Israel Science Foundation (grant No. ISF-2176/19).

Author Contributions

N.M. carried out the experiments and analyzed data. Y.H., U.Y., Y.P., T.T., I.F.L., I.K., L.B., O.D., O.Z., M.B., A.R., and I.V.L. conceived the experiments and interpreted the data. M.B., A.R., and I.V.L. were responsible for financial support. N.M., A.R., and I.V.L. led the writing of the manuscript, in which all coauthors were eventually involved, and approved the submitted version.

Disclosures

The authors have nothing to disclose.

Data Availability

Plasma sequencing data are available from the Gene Expression Omnibus (GEO) repository (accession No.

GSE240273; https://www.ncbi.nlm.nih.gov/geo/query/acc.cgi? acc=GSE240273).

References

1. Obesity. Accessed June 19, 2023. https://www.who.int/health-topics/obesity#tab=tab_1.
2. Breuhl Smith K, Seth Smith M. Obesity Statistics. *Prim Care*. 2016;43:121-35.
3. Ruggiero AD, Key CCC, Kavanagh K. Adipose tissue macrophage polarization in healthy and unhealthy obesity. *Front Nutr*. 2021;8:625331.
4. Pischon T, Boeing H, Hoffmann K, *et al*. General and abdominal adiposity and risk of death in Europe. *N Eng J Med*. 2008;359(20):2105-2120.
5. Pincu Y, Yoel U, Haim Y, *et al*. Assessing obesity-related adipose tissue disease (OrAD) to improve precision medicine for patients living with obesity. *Front Endocrinol (Lausanne)*. 2022;13:860799.
6. Klöting N, Fasshauer M, Dietrich A, *et al*. Insulin-sensitive obesity. *Am J Physiol Endocrinol Metab*. 2010;299(3):E506-EE51.
7. Kawai T, Autieri MV, Scalia R. Adipose tissue inflammation and metabolic dysfunction in obesity. *Am J Physiol Cell Physiol*. 2021;320(3):C375-C391.
8. Odegaard JI, Ricardo-Gonzalez RR, Goforth MH, *et al*. Macrophage-specific PPARgamma controls alternative activation and improves insulin resistance. *Nature*. 2007;447(7148):1116-1120.
9. Watanabe Y, Nagai Y, Honda H, *et al*. Bidirectional crosstalk between neutrophils and adipocytes promotes adipose tissue inflammation. *FASEB J*. 2019;33(11):11821-11835.
10. Goldstein N, Kezerle Y, Gepner Y, *et al*. Higher mast cell accumulation in human adipose tissues defines clinically favorable obesity sub-phenotypes. *Cells*. 2020;9(6) 1508.
11. Čejková S, Lesná IK, Froněk J, *et al*. Pro-inflammatory gene expression in adipose tissue of patients with atherosclerosis. *Physiol Res*. 2017;66(4):633-640.
12. Medzhitov R. The spectrum of inflammatory responses. *Science*. 2021;374(6571):1070-1075.
13. Hardy OT, Perugini RA, Nicoloro SM, *et al*. Body mass index-independent inflammation in omental adipose tissue associated with insulin resistance in morbid obesity. *Surg Obes Relat Dis*. 2011;7(1):60-67.
14. Bartel DP. Metazoan MicroRNAs. *Cell*. 2018;173(1):20-51.
15. Ho JH, Ong KL, Cuesta Torres LF, *et al*. High density lipoprotein-associated miRNA is increased following roux-en-Y gastric bypass surgery for severe obesity. *J Lipid Res*. 2021;62:100043.
16. Park JH, Kornfeld JW. Exomirs at the crossroads-divergent role of exosomal miRNAs in early and chronic obesity. *Nat Metab*. 2021;3(9):1137-1138.
17. Brandao BB, Lino M, Kahn CR. Extracellular miRNAs as mediators of obesity-associated disease. *J Physiol*. 2022;600(5):1155-1169.
18. Thomou T, Mori MA, Dreyfuss JM, *et al*. Adipose-derived circulating miRNAs regulate gene expression in other tissues. *Nature*. 2017;542(7642):450-455.
19. Witwer KW. Circulating MicroRNA biomarker studies: pitfalls and potential solutions. *Clin Chem*. 2015;61(1):56-63.
20. El-Daly SM, Gouhar SA, Abd Elmageed ZY. Circulating microRNAs as reliable tumor biomarkers: opportunities and challenges facing clinical application. *J Pharmacol Exp Ther*. 2023;384(1):35-51.
21. Goldstein N, Tsuneki H, Bhandarkar N, *et al*. Human adipose tissue is a putative direct target of daytime orexin with favorable metabolic effects: A cross-sectional study. *Obesity (Silver Spring)*. 2021;29(11):1857-1867.
22. Mechanick JI, Apovian C, Brethauer S, *et al*. Clinical practice guidelines for the perioperative nutrition, metabolic, and nonsurgical support of patients undergoing bariatric procedures—2019 update: cosponsored by American association of clinical endocrinologists/American college of endocrinology, the obesity society, American society for metabolic and bariatric surgery, obesity medicine association, and American society of anesthesiologists. *Obesity (Silver Spring)*. 2020;28(4):O1-O58.
23. Son DH, Lee HS, Lee YJ, Lee JH, Han JH. Comparison of triglyceride-glucose index and HOMA-IR for predicting prevalence and incidence of metabolic syndrome. *Nutr Metab Cardiovasc Dis*. 2022;32(3):596-604.
24. Giavarina D, Lippi G. Blood venous sample collection: recommendations overview and a checklist to improve quality. *Clin Biochem*. 2017;50(10-11):568-573.
25. Neville MJ, Collins JM, Gloyn AL, McCarthy MI, Karpe F. Comprehensive human adipose tissue mRNA and MicroRNA endogenous control selection for quantitative real-time-PCR normalization. *Obesity*. 2011;19(4):888-892.
26. Makarenkov N, Haim Y, Yoel U, *et al*. Supplementary data for: Circulating miRNAs detect high versus low visceral adipose tissue inflammation in patients living with obesity. Published online August 8, 2023. https://doi.org/10.5281/zenodo.8228599.
27. Shah JS, Soon PS, Marsh DJ. Comparison of methodologies to detect low levels of hemolysis in serum for accurate assessment of serum microRNAs. *PLoS One*. 2016;11(4):e0153200.
28. Martin M. Cutadapt removes adapter sequences from high-throughput sequencing reads. *EMBnet J*. 2011;17(1):10-12.
29. Patil AH, Halushka MK. Mirge3.0: a comprehensive microRNA and tRF sequencing analysis pipeline. *NAR Genom Bioinform*. 2021;3(3):lqab068.
30. Love MI, Huber W, Anders S. Moderated estimation of fold change and dispersion for RNA-Seq data with DESeq2. *Genome Biol*. 2014;15(12):550.
31. Donati S, Ciuffi S, Brandi ML. Human circulating miRNAs real-time qRT-PCR-based analysis: an overview of endogenous reference genes used for data normalization. *Int J Mol Sci*. 2019;20(18):4353.
32. Pizzamiglio S, Zanutto S, Ciniselli CM, *et al*. A methodological procedure for evaluating the impact of hemolysis on circulating microRNAs. *Oncol Lett*. 2017;13(1):315-320.
33. TissueAtlas. Accessed August 2, 2023. https://ccb-web.cs.uni-saarland.de/tissueatlas2/.
34. Wajchenberg BL. Subcutaneous and visceral adipose tissue: their relation to the metabolic syndrome. *Endocr Rev*. 2000;21(6):697-738.
35. Sun X, Icli B, Wara AK, *et al*. MicroRNA-181b regulates NF-κB-mediated vascular inflammation. *J Clin Invest*. 2012;122(6):1973-1990.
36. Sun X, Lin J, Zhang Y, *et al*. MicroRNA-181b improves glucose homeostasis and insulin sensitivity by regulating endothelial function in white adipose tissue. *Circ Res*. 2016;118(5):810-821.
37. Wang Y, Zhu K, Yu W, *et al*. MiR-181b regulates steatosis in non-alcoholic fatty liver disease via targeting SIRT1. *Biochem Biophys Res Commun*. 2017;493(1):227-232.
38. Chen Y, Lin D, Shi C, *et al*. MiR-3138 deteriorates the insulin resistance of HUVECs via KSR2/AMPK/GLUT4 signaling pathway. *Cell Cycle*. 2021;20:353-368.
39. Zhu Z, Rong Z, Luo Z, *et al*. Circular RNA circNHSL1 promotes gastric cancer progression through the miR-1306-3p/SIX1/vimentin axis. *Mol Cancer*. 2019;18(1):126.
40. He ZJ, Li W, Chen H, Wen J, Gao YF, Liu YJ. miR-1306-3p targets FBXL5 to promote metastasis of hepatocellular carcinoma through suppressing snail degradation. *Biochem Biophys Res Commun*. 2018;504(4):820-826.
41. Wu YY, Wang Q, Zhang PA, Zhu C, Xu GY. miR-1306-3p directly activates P2X3 receptors in primary sensory neurons to induce visceral pain in rats. *Pain*. 2023;164(7):1555-1565.
42. Keller A, Meese E. Can circulating miRNAs live up to the promise of being minimal invasive biomarkers in clinical settings? *Wiley Interdiscip Rev RNA*. 2016;7(2):148-156.
43. Huang DW, Sherman BT, Lempicki RA. Systematic and integrative analysis of large gene lists using DAVID bioinformatics resources. *Nat Protoc*. 2008;4(1):44-57.